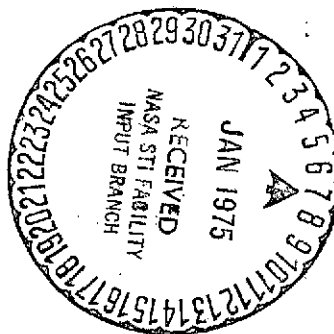PERFORMANCE CHARACTERISTICS OF A HELIUM-3 COOLED
SEMICONDUCTOR BOLOMETER FOR ASTRONOMICAL
INFRARED SPECTROSCOPY

R. Katterloher

Translation of: "Anforderungen an ein
Helium 3 gukuehltes Halbleiter-bolometer
fur astronomische Infrarot-Spektroskopie,"
Max Planck Institute for Physics and
Astrophysics, MPI-PAE/TB Extraterrestrial
14, August 1974, Munich.

NATIONAL AERONAUTICS AND SPACE ADMINISTRATION
WASHINGTON, D. C. 20546   DECEMBER 1974

1. Report No. NASA TT F 16,077	2. Government Accession No.	3. Recipient's Catalog No.
4. Title and Subtitle PERFORMANCE CHARACTERISTICS OF A HELIUM-3 COOLED SEMICONDUCTOR BOLOMETER FOR ASTRONOMICAL INFRARED SPECTROSCOPY		5. Report Date 26 December 1974
		6. Performing Organization Code
7. Author(s) R. Katterloher		8. Performing Organization Report No.
		10. Work Unit No.
9. Performing Organization Name and Address SCITRAN Box 5456 Santa Barbara, CA 93108		11. Contract or Grant No. NASw-2483
		13. Type of Report and Period Covered Translation
12. Sponsoring Agency Name and Address National Aeronautics and Space Administration Washington, D.C. 20546		14. Sponsoring Agency Code

15. Supplementary Notes

Translation of: "Anforderungen an ein Helium 3 gukuehltes Halbleiter-bolometer für astronomische Infrarot-Spectroskopie, Max Planck Institute for Physics and Astrophysics, MPI-PAE/TB Extraterrestrial 14, August 1974, Munich.

16. Abstract

A number of instruments are considered and analyzed for a high-altitude infared spectroscopy balloon experiment (bolometers, photosemiconductors, Josephson detectors, pyroelectrical detectors). Various noise sources are considered (noise due to current fluctuations, photon noise, phonon noise, thermal noise, generation-recombination noise, flicker noise). Operational data are calculated for a bolometer (resistance dependence on temperature, responsivity, NEP, frequency variation) and a design analysis is made. A design for a Helium-3 cryostat is given.

17. Key Words (Selected by Author(s))	18. Distribution Statement Unclassified – Unlimited

19. Security Classif. (of this report) Unclassified	20. Security Classif. (of this page) Unclassified	21. No. of Pages 40	22. Price

ii

CONTENTS

PERFORMANCE CHARACTERISTICS OF A HELIUM-3 COOLED SEMICONDUCTOR BOLOMETER FOR ASTRONOMICAL INFRARED SPECTROSCOPY

R. Katterloher*

1. Introduction

Spectroscopy measurements of infrared radiation in a range   /1**
between 100 μm and 1000 μm requires detectors with uniform
spectral sensitivity if the Fourier interferometry method is
used. At the present time, only bolometers can be used as
sensitive IR detectors with such wide band response capacity.
Photosemiconductors, Josephson detectors, and pyroelectrical
detectors do exceed bolometers in certain charactersitics, but
can only be used optimally in a wavelength range which is too
limited for Fourier spectroscopy. Since the detection effect
of a bolometer is based on the change of an electrical resistance
because of temperature increase caused by the absorbed IR
radiation, a careful adaptation of the electrical, thermal, and
optical properties must be made for each application.

2. Measurement Principle

For the present application [1] [8], it seems that a He 3
cooled semiconductor bolometer with a p dose germanium monocrystal
is most promising. Semiconductor bolometers have lower self-
noise compared with charcoal layer bolometers for comparable

**Numbers in the margin indicate pagination of original
foreign text.

boundary conditions and also have increased detectivity. By the detectivity D, we mean the reciprocal of the equivalent noise power NEP (W/√Hz) or the ratio of response capacity r (responsivity) to the effective noise voltage N.

$$D = \frac{1}{NEP} = \frac{r}{N} \qquad \frac{(V/W)}{(V/\sqrt{Hz})}$$

(1) /2

The NEP value of a detector, therefore, specifies the amount of detectable radiation energy for a signal/noise ratio = 1 and for a bandwidth of 1 Hz (or 1 second integration time).

As the temperature drops, the resistance of the semiconductor material increases drastically. In order to provide large signal voltages, large temperature coefficients are desirable. The resistance dependence of germanium can be represented according to [2] and [3] according to the relationship

$$R(T) = k \cdot e^{B/T}$$

(2)

(where k and B are constants). According to [4], [5], and [10], the following relationship is accurate enough:

$$R(T) = R_o \left(\frac{T_o}{T}\right)^A$$

(3)

where R_o is the resistance of the element at T_o and A is a constant which depends on the dosing (and the temperature) with values between A = 1 and A = 9. It is determined with measured R-T curves and one usually finds A ≈ 4, see Figure 1. The temperature coefficient α is given by

$$\alpha = 1/R \cdot dR/dT$$

(4)

From this, we find by substitution of (2),
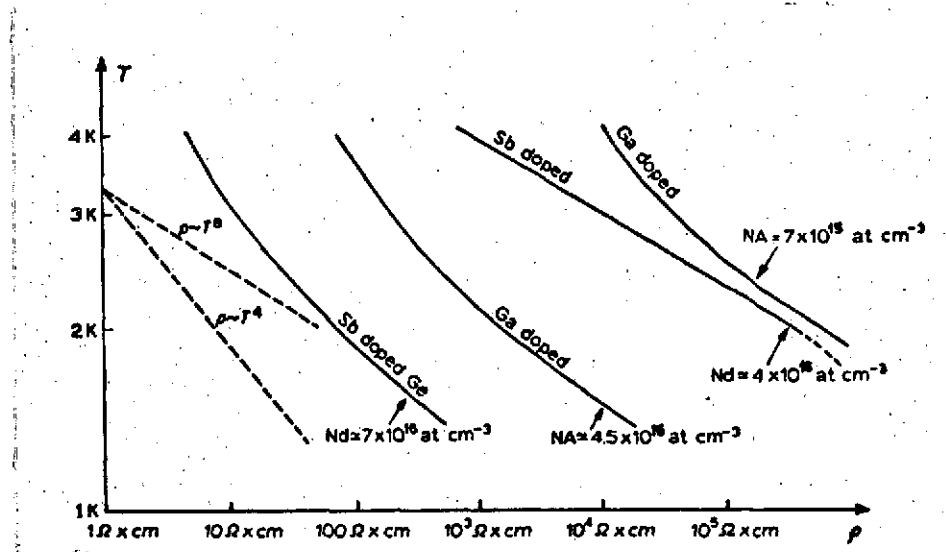
$$\alpha = - B/T^2$$

(5)

Figure 1. Temperature dependence of specific resistance [4].

and by substituting (3) /3

$$\alpha = -A/T \qquad (6)$$

By reducing the temperature, we can always find a larger α.
For the further calculation, we will use the relationship (6).

The energy Q absorbed by the bolometer can be divided into three parts:

a) the (modulated) useful signal Q_s,

b) the constant perturbation radiation of the bolometer surroundings (optical system, background radiation) Q_n,

c) the Joule heating Q_J caused by the measurement current.

We find

$$Q = Q_s + Q_n + Q_J \qquad (7)$$

3

In order to maintain the detector at a constant temperature T, the power must be removed by means of a certain heat conductivity value G to a cold bath having the temperature T_B.

$$Q = G(T - T_B)$$ (8)

In general, of the components Q_s, Q_n, and Q_J, the magnitude of Q_s will be the smallest (in the present case, typically 10^{-13} W). Q_n is larger (10^{-7} W), and Q_J is the largest of all (10^{-6} W) typically). The effect of constant perturbation radiation, therefore, brings about a reduction in the detector performance capacity because it increases the working temperature of the bolometer even more above the bath temperature. This magnitude will be ignored, compared with Q_J in the following. Q_J cannot be decreased arbitrarily, because otherwise the signal voltages produced are too small. For the same reason (in addition to other boundary conditions), one is limited in the variation G. In the stationary case, we have approximately

$$G(T - T_B) = Q_J$$ (9)

The voltage U(T) applied to the bolometer and the measurement current J(T) can be expressed as follows as a function of Q_J.

$$U(T) = \sqrt{R(T)Q_J} = \left[R(T)G(T - T_B)\right]^{1/2}$$ (10)

$$J(T) = \sqrt{R^{-1}(T)Q_J} = \left[R^{-1}(T)G(T - T_B)\right]^{1/2}$$ (11)

where it has been assumed that, for the load resistor, we have /5 $R_L \gg R$ and G does not depend on detector temperature.

4

The responsivity of the bolometer for the quasi-stationary operation is found as a ratio of the voltage per degree of temperature and the difference of thermal conductivity (W/K), minus the produced Joule heat per degree [5], [10]:

$$r = \frac{U}{(G - \alpha \cdot Q_J)} \qquad \frac{V}{W} \tag{12}$$

By substituting (6), (9), and (10) in (12), we find the following relationship between r and T

$$r(T) = \frac{(-A/T)(T-T_B)^{1/2} \cdot R(T)^{1/2}}{[1 + (A/T)(T-T_B)] \cdot G^{1/2}}$$

and because of (3), we find

$$r(T, T_B) = \left[\frac{-(A/T)(T-T_B)^{1/2}}{1 + (A/T)(T-T_B)} \right] \left[\frac{R_B (T_B/T)^A}{G(T_B)} \right]^{1/2} \tag{13}$$

If we introduce $T/T_B = \vartheta$, we find

$$r(\vartheta) = -\left[\frac{A^2 (\vartheta - 1)}{[\vartheta(1+A) - A]^2 \cdot \vartheta^A} \right]^{1/2} \left[\frac{R_B}{T_B \cdot G(T_B)} \right]^{1/2} \tag{14}$$

For a specified bath temperature T_B and prescribed A (crystal properties), Equation (14) defines the dependence of responsivity [/6] on the bolometer temperature T or ϑ. Figure 2 shows that, for different A, there exist different maxima of r as a function of ϑ. In principle, r increases when T_B and $G(T_B)$ are reduced.

The time constant τ of a bolometer is given by

$$\tau = C/(G - \alpha Q_J) \tag{15}$$

where C is the heat capacity of the detector. By substituting Equations (6), (9), and $\vartheta = T/T_B$, we find
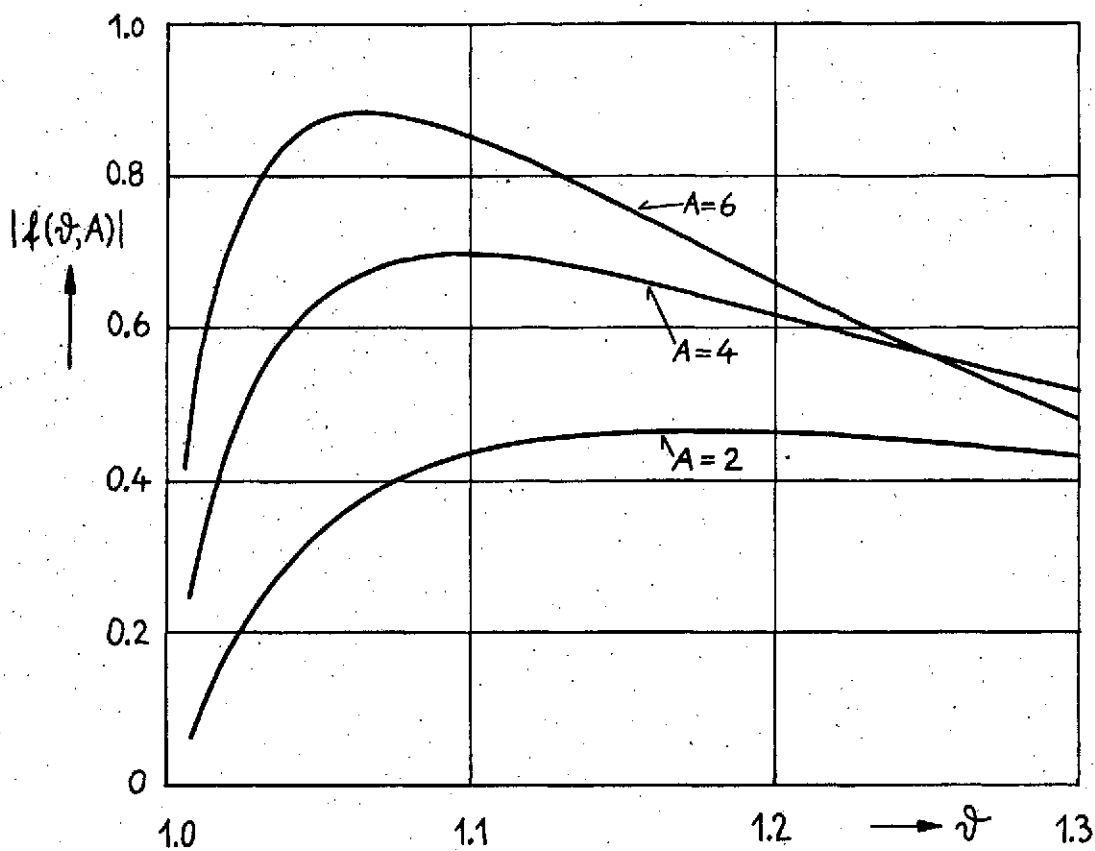
/7

5

Figure 2. Influence of A and ϑ on responsivity.

$$\tau = \frac{C}{G} \cdot \frac{1}{1 + A\,(1 - 1/\vartheta)} \qquad (16)$$

The time constant, therefore, has a factor which depends on A and ϑ, similar to the responsivity. For A = 4, we find a factor of 0.7 for optimum ϑ for both quantities. Equation (16), however, does not have a maximum and large A always has a favorable effect.

6

3. Noise Mechanisms and Maximum Detectivity

Since the detectivity depends on the responsivity *and* the noise voltage of the detector, we must investigate the ϑ value at which the NEP takes on a minimum or when the detectivity takes on a maximum. The noise mechanisms which are effective at the bolometer consist of the following:

a) noise caused by various types of current fluctuations,

b) photon noise caused by background radiation which cannot be completely suppressed,

c) phonon noise caused by thermal coupling with the cold bath.

Regarding c), the noise caused by phonon fluctuation is given by the following in [7]

$$W_{Phonon} = [2 k G (T^5 + T_B^5)/T^3]^{1/2}$$
$$\approx [4 k T_B^2 G (T_B)]^{1/2} \quad W/\sqrt{Hz} \tag{17}$$

(where k = Boltzmann constant) and for a germanium element with /8 a volume of 0.5 mm³ and a time constant of $\tau \approx 1$ ms $(G \approx 1 \cdot 10^{-7}$ W/K) with a bath temperature of about 0.3° K, is

$$W_{Phonon} \approx 1 \cdot 10^{-15} \ W/\sqrt{Hz}.$$

By reducing G, which is only possible by reducing C for a given τ, the phonon noise can be reduced so much until it no longer dominates as a noise source.

Regarding b), the photon noise in the thermal radiation from the surfaces of the optical system and of the background make up another contribution for the total noise power in the detector and, according to [2], it is calculated from

$$W_{Photon} = \frac{h}{c} \left[2 F \Omega \Delta f \, \varepsilon \int_0^\infty \frac{\nu^4 \, e^{h\nu/kT} \, d\nu}{(e^{h\nu/kT} - 1)^2} \right]^{1/2}, \; W \qquad (18)$$

(h = Planck constant, c = speed of light, F = emitting area, Ω = solid angle, Δf = bandwidth of measurement unit, ε = emissivity of surface, ν = frequency, and T = temperature). In Figure 3, we show the intensity distribution [integrand of Equation (18)]. The curves show that, depending on temperature of the radiating body, substantial amounts of the noise spectrum can be removed from the measurement range by means of optical filters. Only radiators, which are at the temperature of liquid nitrogen will almost exclusively radiate their noise power in the measurement range in question, so that in this case, not much can be done by using (wideband) filters.

If we integrate over all frequencies, then (18) can be expanded as a function of $T^{5/2}$ by integral decomposition. The noise power W_{Photon} for a grey body is related to the radiation intensity which produces it (background radiation) Q_n in the following way [8]:

$$W_{Photon} = (4 \, k \, T_n \, Q_n)^{1/2} \qquad W/\sqrt{Hz} \qquad (18a) \quad \text{/10}$$

For an emission factor of $\varepsilon = 0.02$, Figure 4 shows the noise power produced by a surface with $F \cdot \Omega = 5.5 \cdot 10^{-4} \, sr/cm^2$.

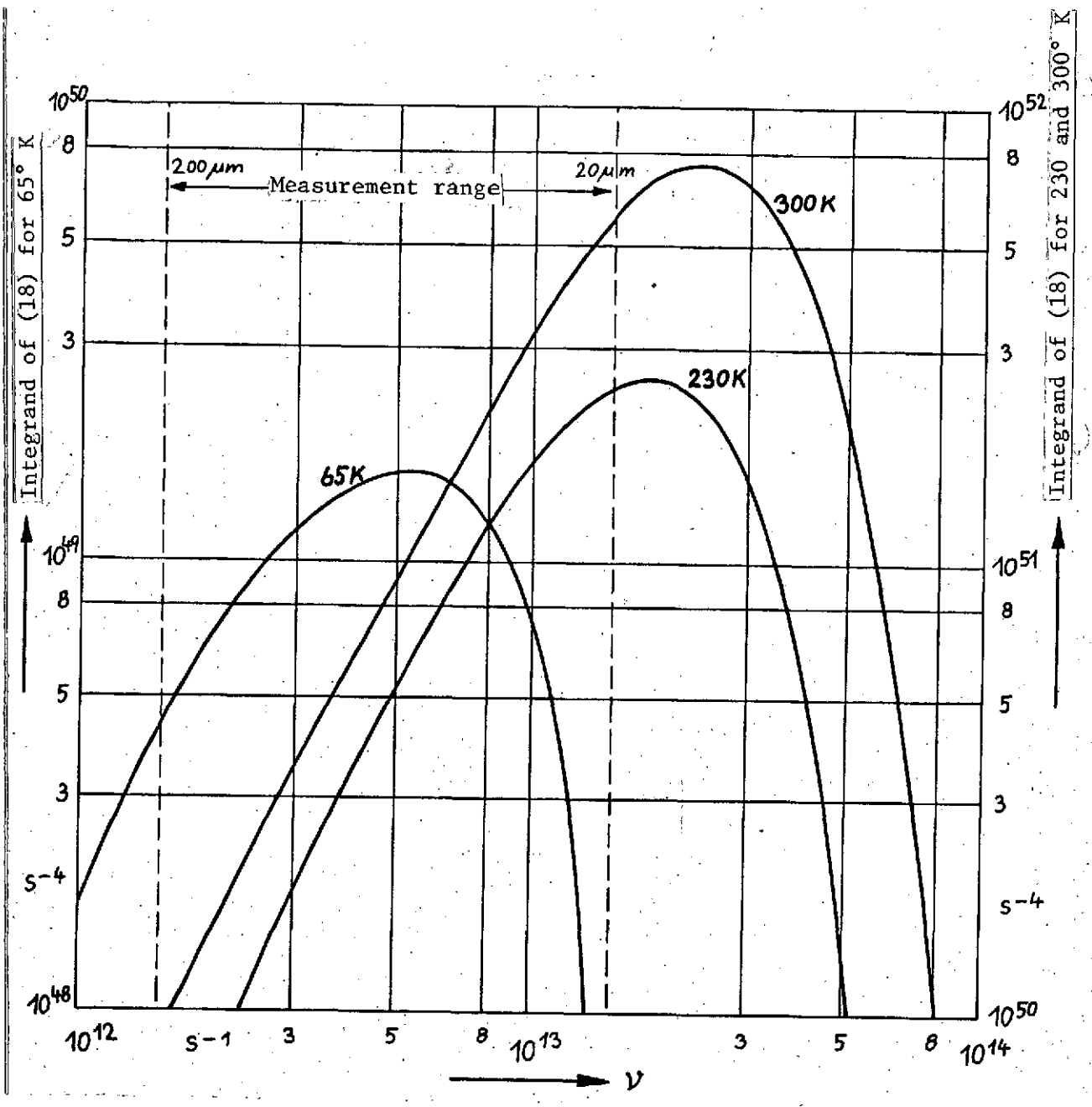Figure 3. Noise spectra for various temperatures.

Point A is reached with ideal filtering with 20 μm < λ < 200 μm. Point B is obtained with a bandpass of 20 μm < λ < 30 μm, and Point C with a 2 μm width around 28.5 μm.
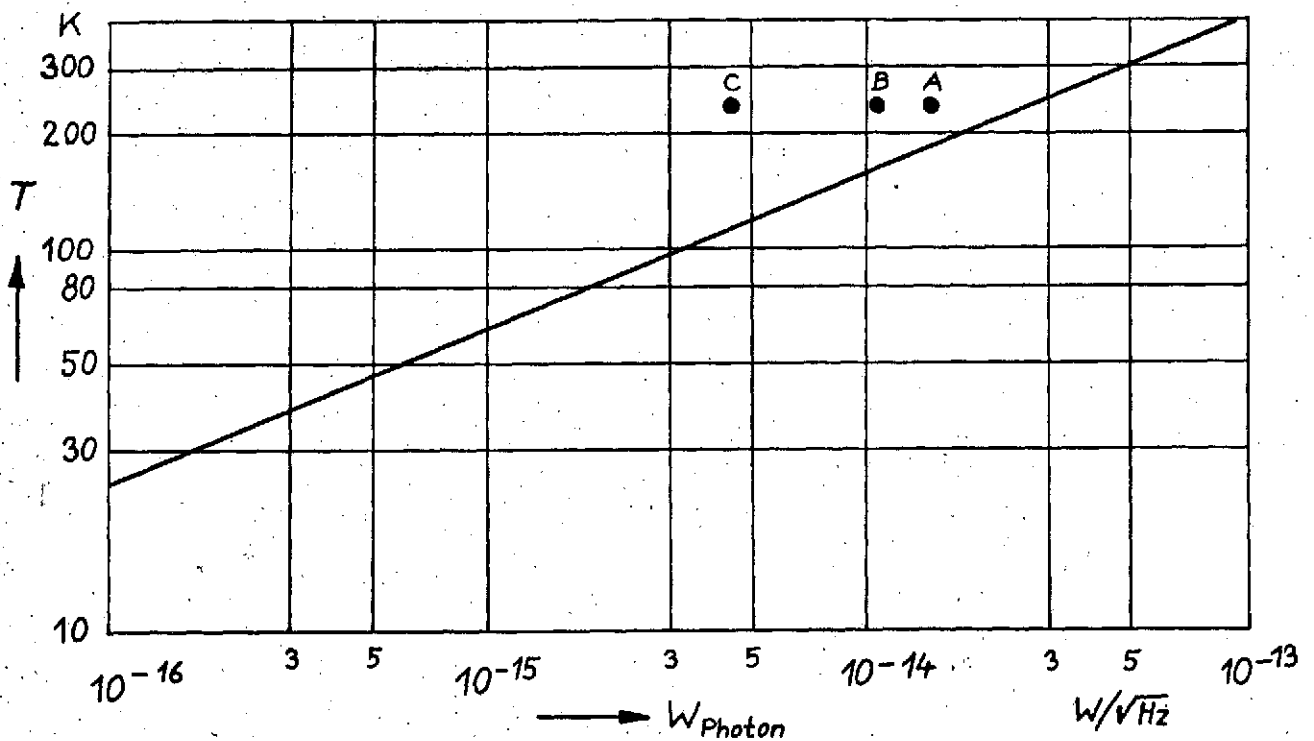
Figure 4. Photon noise.

If we want to have available the entire measurement range
between 20 and 200 μm, then the only filters of practical
interest will be those which cut off the shortwave radiation,
i.e., wavelengths below 20 μm. By blocking off the radiation
from 200 μm to ∞, one obtains a gain which can be ignored in
the present application. The following materials could be
used, for example, [9]:

— sapphire with diamond dust, 1 mm thick, transmission
about 60%, cut-on wavelength 27 μm;

— CaF₂ with polyethylene and diamond dust, 1 mm thick,
transmission about 70%, cut-on wavelength 50 μm.

As a window material (vacuum sealing), we can use black polyethylene foil, 0.1 mm thick, transmission about 90%, emissivity about 5%.

The filters must be cooled to the temperature of liquid helium, because some of the spectral properties mentioned above only occur under these conditions and if the temperature is higher, they could reduce the detection capacity of the detector because of their eigen emission. In addition, the absorbed part of the thermal background radiation must be transferred to the cold bath. A filter with a cut-on of 27 μm (ideal) will hold away about 75% of the incident atmospheric radiation (230° K). We would also like to mention that the maximum thermal emission of a gray body does not occur at the same wavelength as its maximum noise intensity. For a 230° K radiator, the maximum noise is located at 17 μm and the maximum radiation — at 13 μm.

Regarding a), the noise components produced in the bolometer itself are composed of the following [6], [11]:

— thermal noise,

— generation-recombination noise,

— 1/f noise.

The thermal noise (Johnson noise or Nyquist noise) is caused by fluctuations of the velocity vectors of the electrons. The dependence of the noise voltage N on temperature for such an electron gas is given by

$$N = (4kTR \, \Delta f)^{1/2} \qquad V \qquad \qquad (19)$$

Johnson noise does not depend on frequency.

The generation-recombination noise is a consequence of the charge carriers generated and recombining at the defects of the semiconductor, which occur statistically and have an average lifetime of τ_0. The noise intensity $(\Delta J)^2$ is found as

$$(\Delta J)^2_{GR} = K J^2 \Delta f / (1 + (2\pi f \tau_0)^2) \qquad A^2 \qquad (20)$$

The generation-recombination noise is proportional to the square of the current J and is practically "white" up to an inflection frequency $f_0 = 1/2\pi\tau_0$, and after this, it drops off accourding to $1/f^2$. Because of $\tau_0 \approx 10^{-6}$, the limiting frequency is usually in the megahertz range.

The 1/f noise (flicker noise or excess noise) is given this name because its intensity is inversely proportional to the frequency. It is caused by the continuous distribution of the charge carrier lifetimes between two limits, τ_1 and τ_2. When the probability for a certain time constant is inversely /13 proportional to τ, the resulting distribution of noise intensity among the individual frequencies is given by

$$v(f) \sim \int_{\tau_1}^{\tau_2} g(\tau) \frac{\tau}{1 + (2\pi f \tau)^2} d\tau \qquad (21)$$

[g(τ) weighting factor for noise intensity with time constant τ].

Between the frequencies determined by τ_1 and τ_2, the noise intensity varies according to 1/f. For lower ones, it remains constant and for higher frequencies, it drops off with $1/f^2$. Theoretical and experimental investigations confirm the fact that this noise mechanism is a *surface effect* (contact problems). Models for this are the tunnel model, the recombination center distribution, or the diffusion model, at the present time.

Experimental investigations on the frequency dependence of the noise intensities in semiconductor bolometers are only given in [14]. The results cannot be considered to have general validity. [2] and [5] consider only the noise components of thermal noise for the design of a bolometer.

Considering Johnson noise, we find the following for the detectivity, according to Equations (1), (14), and (19):

$$D = \frac{r}{N}$$

$$|D| = \left[\frac{A^2 (\vartheta - 1)}{[\vartheta (A+1) - A]^2 \, \vartheta^A} \right]^{1/2} \left[\frac{R_B}{T_B \, G(T_B)} \right]^{1/2} \left[4kTR \cdot \Delta f \right]^{-1/2} \quad (22)$$

With $T = \vartheta \cdot T_B$ and $R = R_B \cdot \vartheta^{-A}$, we find   /14

$$|D| = \left[\frac{A^2 (\vartheta - 1)}{[\vartheta (A+1) - A]^2 \cdot \vartheta} \right]^{1/2} \cdot \left[\frac{1}{4 \, k \, T_B^2 \, G(T_B) \Delta f} \right]^{1/2} \quad (23)$$

Accordingly, the detectivity is proportional to $1/T_B$ and $1/\sqrt{G}$. The dependence of the overtemperature $|\vartheta|$ of the bolometer compared with the bath temperature and the resistance variation R(A) is given in Figure 5.

The maxima of the function is found from the condition   /15
$dD/d\vartheta = 0$ or from the cubic equation

$$\vartheta^3 (-2A^2 - 4A - 2) + \vartheta^2 (5A^2 + 8A + 3) +$$
$$\vartheta(-4A^2 - 4A) + A^2 = 0 \quad (24)$$

For A = 4, we find $\vartheta_{max} \approx 1.13$, i.e., the bolometer temperature should lie about 1/8 above the bath temperature. Slightly different ϑ values produce practically no deterioration
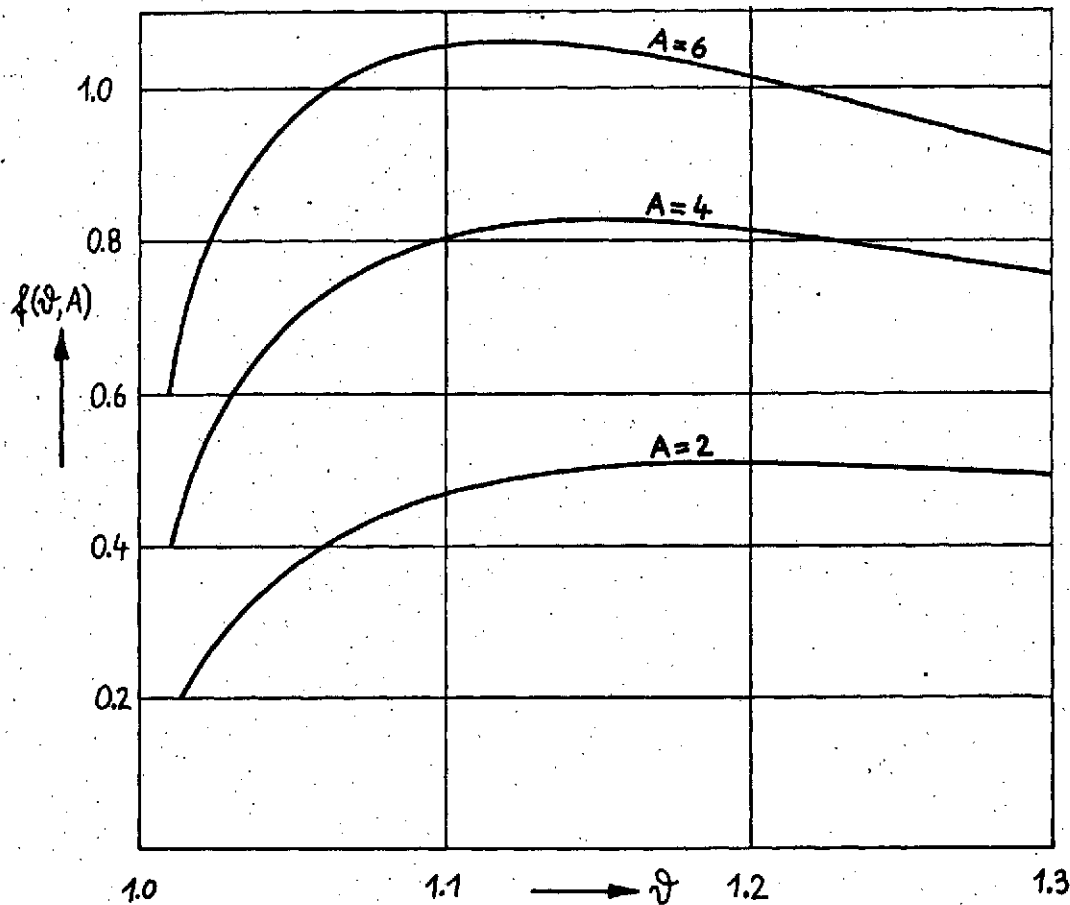
Figure 5.   Influence of overtemperature $|\vartheta|$ on detectivity.

of D or r because of the flat curve variation.   The operational values of a bolometer, therefore, should provide for maintaining $|\vartheta_{max}|$, if the greatest possible sensitivity is desired.

With $T_B = 0.3°$ K and $G = 1 \cdot 10^{-7}$ W/K, we were theoretically able to obtain a detectivity of 10^{15} $\sqrt{Hz}$/W for a time constant of 1 msec.   Together with the phonon noise (17), this results in a NEP of $|\lesssim 2 \cdot 10^{-15}$ W/$\sqrt{Hz}|$.   We have

$$NEP \approx \left[(W_{Phonon})^2 + (1/D)^2 \right]^{1/2} \quad W/\sqrt{Hz} \qquad (1a)$$

This sensitivity can only be exploited if the noise power of the background radiation remains small, i.e., for a corresponding cooling of the bolometer surroundings and of the optical system and/or by using filters which are also cooled, which intersect the noise spectrum (see Sections 3/4).

4. Determination of Operational Data

Under practical conditions, the operational data of the bolometer are determined as follows: for the lowest possible current load and for the best possible coupling between the crystal and the cold gas, one measures the resistance dependence R(T) of the bolometer by varying the temperature. Using Equation (3), we obtain A. The dependence of U on I (load curve) is determined with operational conditions (without a signal). The heat conductivity coefficient G is found in the form of a differential, according to Equation (9)

$$G = dQ_J/dT = \frac{dQ_J/dR}{dR/dT} \qquad (9a)$$

It is now necessary to determine the two quotients dQ_J/dR and dR/dT. Since U(I) is known, we find from this $Q_J(I) = I \cdot U(I)$ and R(I) = U(I)/I. The derivatives of both functions dQ_J/dI and dR/dI lead to the desired quotient dQ_J/dR at a selected point I. From the given R(I) variation, we find the R which belongs to this I. The inverted equation (3), for which the constant is now known, produces the dependence dR/dT as a function of R

$$dR/dT = \frac{-A}{T_o R_o^{1/A}} \cdot R^{1 + 1/A} \qquad (4a)$$

so that G can now be calculated from (9a).

The responsivity could be determined using Equation (14) for optimum ϑ. However, we still do not have the value of I at which the optimum ϑ occurs. Therefore, the dependence of the responsivity on the measurement current I is desired. According to [2], we have

$$r = I(dR/dQ_J)$$ (25)

[7], [10], [11], and [14] use the corresponding relationship

$$r = (dU/dI - R)/2U$$ (26)

From the measured U-I variation, we can determine the values of dR/dQ_J or dU/dI, respectively, they are already known for determining G. Therefore, r(I) has been found by experiment. Figure 6 shows these measured curves for a Ge bolometer [14] at 1.55° K.

The maximum responsivity and minimum NEP are different only by a negligible amount (with respect to ϑ) and, therefore, the I value found here results in the optimum operation point of the bolometer.

The responsivity determined this way is usually called the DC responsivity, because only very slow signal changes produce the above mentioned values. In practice, the incoming signal is usually modulated (chopped), so that there is a greater or lesser reduction of the output signal. The reason for this is the following: a bolometer operates faster, if the heat which causes the temperature increase can be removed faster. In other words, the heat flux Q from the bolometer is responsible for its rapidness of response r. Q is determined by the dynamic conductivity value Y, which is composed of the stationary heat
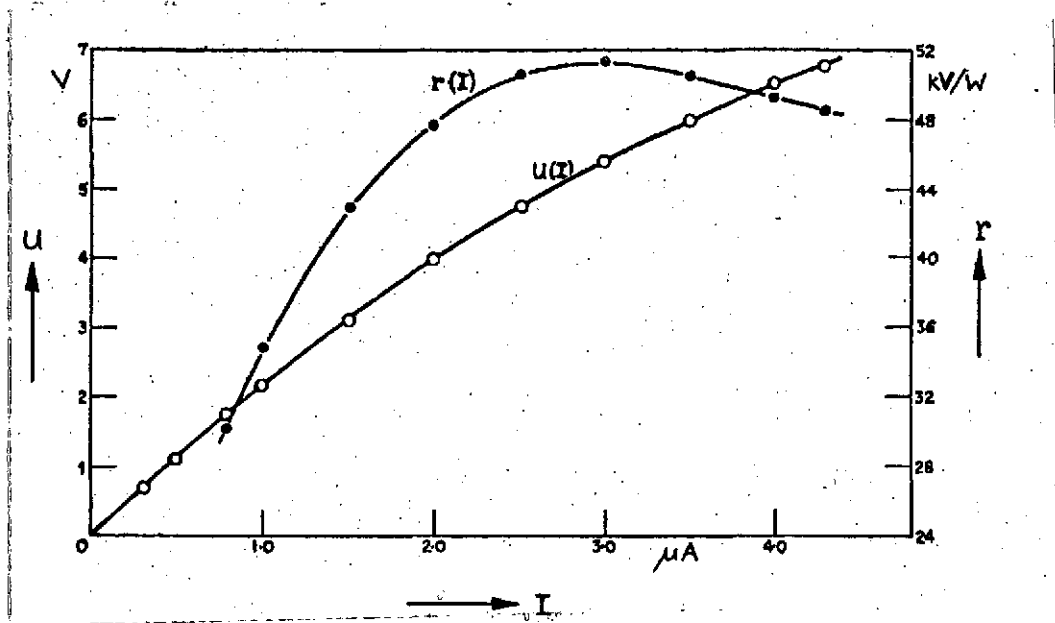
Figure 6. U(I) and r(I) variations for a Ge bolometer.

conductivity value G, as well as the storage capacity C of the crystal:

In order to be able to determine the frequency variation of the bolometer, it is necessary to find the dependence of the conductivity Y on the frequency ω of the temperature fluctuations. The analog procedure for the corresponding electrical circuit provides the following solution:
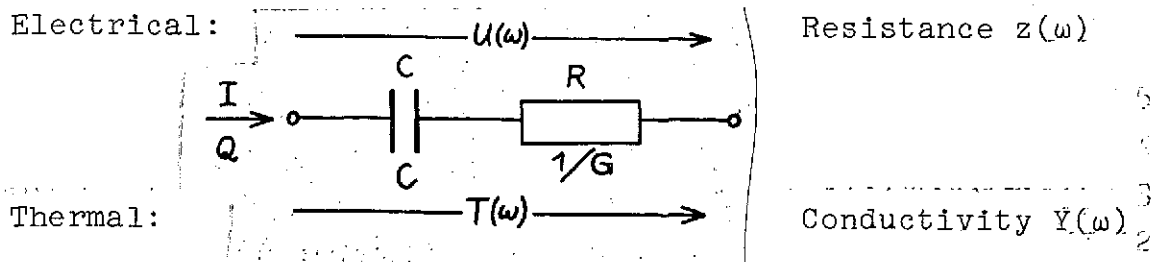
Trial solution for RC series circuit:

$$\zeta = 1/G - j/\omega C$$
$$|\zeta| = \sqrt{\frac{1}{G^2} + \frac{1}{\omega^2 C^2}} = \frac{1}{\omega C}\sqrt{1 + \omega^2 C^2 / G^2}$$

(27)

If we introduce $C/G = \tau$ (time constant of the bolometer), we find the following for $Y(\omega)$

$$Y(\omega) = \frac{1}{|\zeta|} = \omega C \frac{1}{(1 + \omega^2 \tau^2)^{1/2}}$$

(28)

For $\omega \ll 1$, we have $Y_0 = \omega C$, so that

$$Y(\omega) = Y_0 \cdot (1 + \omega^2 \tau^2)^{-1/2}$$

(29)

and, correspondingly, the responsivity $r(\omega)$ is

$$r(\omega) = r_0 \frac{1}{(1 + \omega^2 \tau^2)^{1/2}}$$

(30)

$r(\omega)$ decreases with increasing frequency, which is why one wants the smallest time constants τ possible. This is related to an increase in the NEP, if C cannot be arbitrarily reduced. At the frequency $\omega_k = 1/\tau$, the quantity $r(\omega)$ decreases to the value

$1/\sqrt{2}$ (inflection point). In practice, this maximum frequency will not be exceeded because otherwise, the output signal drops off rapidly. The frequency variation of the responsivity for two different time constants is shown in Figure 7.

For a given bolometer, we determine the time constant τ by measuring the frequency curves (30) or by determining the point ω_k. Using Equation (16), we can first calculate the effective quotient C/G from this. If the dimensions of the bolometer are
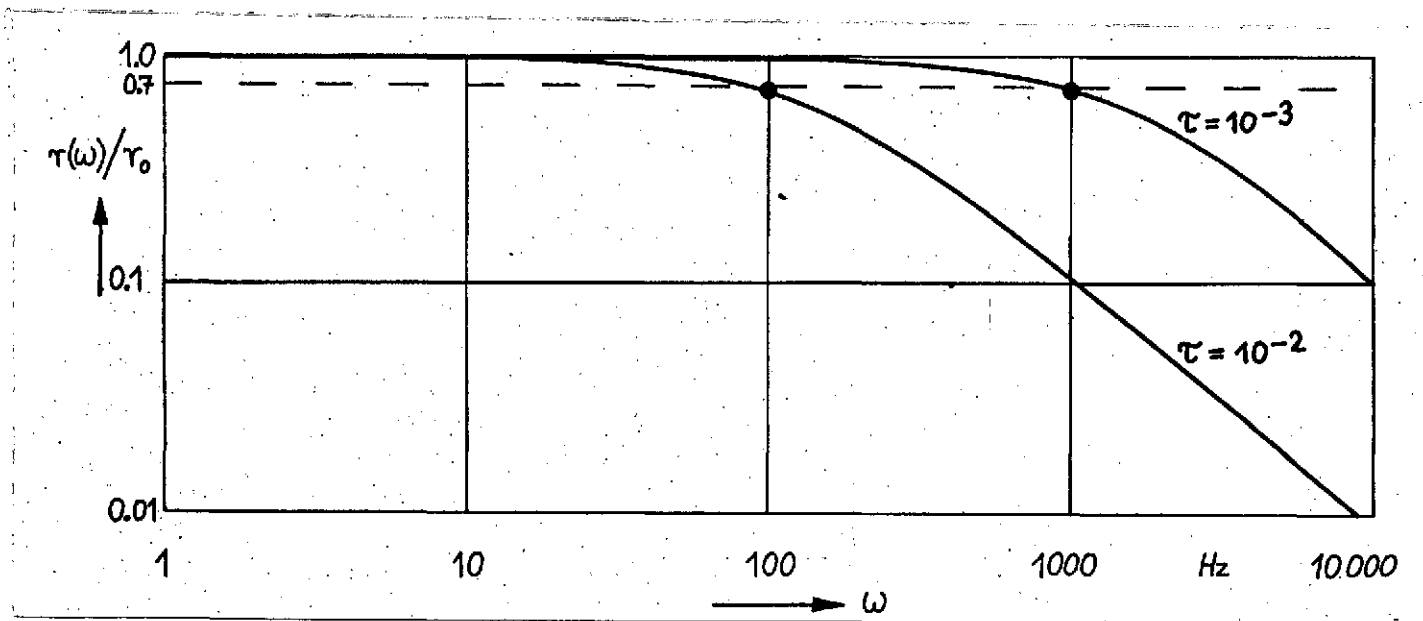
Figure 7. Frequency dependence of responsivity.

known, and if we can ignore the contributions of the connection
wires to the heat capacity of the connector, we find the follow-
ing for C

$$C = 6.8 \cdot 10^{-9} \cdot T^3 \cdot V, \qquad J/K \qquad (31)$$

(where V must be substituted in mm^3 and the Debye temperature
of germanium is 370° K).

From this, G can be calculated and should agree with the
value from Equation (9a). Conversely, from the measured values
of (9a) and the relationships (16) and (31), we can determine
the expected time constant τ.

5. Construction Design

The optics of the planned balloon telescope [8] images the
image of the radiation source on an area with a diameter of
about 3 mm. Since we only plan to first use a bolometer cooled
to 1.5° K, an additional off-axis mirror with a 3.5 mm diameter
and a focal length of 8.4 mm reduces the image to a diameter of
0.7 mm in order to exploit the advantages of a small detector
(NEP ≈ $3 \cdot 10^{-14}$ W/$\sqrt{Hz}$) [12]. With the desirable 0.3° K cooling,
it will not be necessary to retain these small detector dimen-
sions. Apparently, a bolometer with an edge length of 3 mm
also provides the expected improvement in detectivity. This
would then make it possible to eliminate the small mirror and
also several construction features in the bolometer mounting
could be exploited (aperture angle of incoming radiation bundle
about 12°). Since a detector with a diameter of 1 mm and
0.3° K would provide the largest possible experimental sensi-
tivity which would still be reasonable, we will consider this
type as well in the remainder of our discussion.

First of all, we must select a suitable semiconductor material for the measurement element. Based on its optical properties, it should provide 100% absorption of incident radiation, if possible. On the other hand, the electrical values of the detector must allow an optimum adaptation of the measurement chain for signal amplification. For a wavelength range of 20 — 200 µm, we find that p-conducting germanium is very suitable. The type and extent of dosing must be adjusted according to the application. Investigations on the influence of dosing can be found in [13] and [14]. Doubly dosed germanium is found to be favorable, which absorbs over 90% of the IR radiation in the wavelength range of interest here. By means of a thin (5 to 10 µm) "black" layer [4], [12], it is possible to even increase the absorption capacity. The values shown in Figure 8 apply for an element with a thickness of 250 µm at a temperature of 4.2° K, which is dosed with $N_a = 9 \cdot 10^{15}$ cm^{-3} Ga and $N_d = 1 \cdot 10^{15}$ cm^{-3} Sb , corresponding to a compensation ratio of K = N_d/N_a = 0.11. Smaller values of K are not recommended because they reduce the absorption capacity considerably. Also, the reduction in the element thickness has the same effect.

The increase in the electrical conductivity of the crystal by energy absorption is based on thermal activation of the (bound) charge carriers (holes)here) available at the defects. According to Equation (2), the conductivity decreases rapidly when there is a temperature reduction, so that by making available more charge carriers, i.e., by using higher dosing rates, one again attempts to obtain acceptable resistance values for the measurements. Of course, we can finally have "impurity band conduction" here, an effect in which the charge carriers become mobile without thermal activation within a defect conduction band which has formed. However, the bolometer
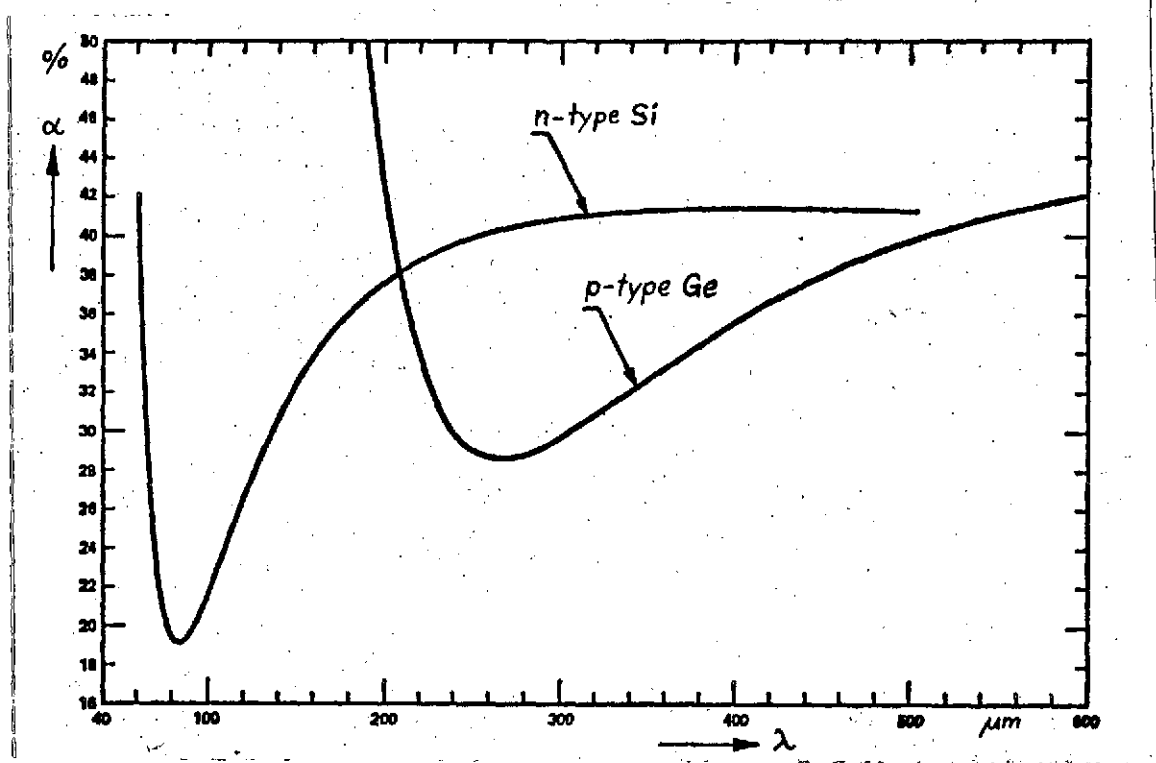
Figure 8. Absorption capacity of Ge and Si [13].

properties of the crystal then are lost. Concentrations of
< 10^{17} cm^{-3} for Ge and < 10^{19} cm^{-3} for Si [14] are still
allowable. The following Table 1 shows specific data of a few
Ge bolometers from [2], [4], [12], and [13], in which it is
possible to determine values which seem suitable for any
application. See the last column.

Using the resistance mentioned above, it is possible to
obtain a resulting total resistance of typically 10^6 Ω for
conventional bolometer dimensions. In order to maintain the
measurement currents sufficiently constant, a 10^7 Ω load
resistor cooled to the He temperature should also be switched
in, in order to suppress noise. Since field strengths of only
5 V/cm are permissible for Ge:Ga, the allowable voltage across

TABLE 1*

PROPERTIES OF p TYPE Ge MONOCRYSTALS

Author	[13]	[12]	[4]	[2]	Here
N_a, cm^{-3}	$9 \cdot 10^{15}$ Ga	$x \cdot 10^{16}$ Ga	$4.5 \cdot 10^{16}$ Ga	$6 \cdot 10^{16}$ In	$8 \cdot 10^{16}$ Ga
N_d, cm^{-3}	$1 \cdot 10^{15}$ Sb	?	?	$2,4 \cdot 10^{16}$ Sb	$2 \cdot 10^{16}$ Sb
K	0.11	0.1 ?	0.1 ?	0.4	0.25
ϱ, Ωcm	10^4	$3 \cdot 10^5$	10^4	10^5	10^5-10^6
at T, K	4.2	1.5	1.5	0.37	0.33

*Commas in the numbers indicate decimal points.

the measurement element must be < 1 V. This brings about a
current of < 1 μA and a loss power of < 1 μW. Responsivity
values are around 10^6 V/W in this case, so that, with the
expected signal powers of $\approx 5 \cdot 10^{-14}$ W, the signal voltages
which occur will be a few 10 nV. If the following amplification
chain has a bandwidth of 10 Hz ($\Delta f \geqslant 200$ Hz is required for
the following rapid scan interferometry), then the produced
noise voltage is about one order of magnitude above the signal
value. This means that, for the required signal/noise ratio
S/N, we have the following condition for the measurement time

$$t_{measurement} = (\frac{S}{N} \cdot \frac{NEP}{Signal})^2 \qquad s \qquad (32)$$

We would like to mention the fact that, in the previously
mentioned application (range $5.5 \cdot 10^{-4}$ sr cm^2), the perturba-
tion radiation of the atmosphere recorded by the detector per
line is found to be $3 \cdot 10^{-10}$ W, and the integral value is
21 — 500 μm [15], as shown in Table 2. Therefore, a signal

TABLE 2*

ATMOSPHERIC DATA

Altitude, km	30	35.	40	45
T, K	230	245	260	270
ε % black body	1.29	0.63	0.31	0.15
Q , W :	$3,6 \cdot 10^{-8}$	$2,3 \cdot 10^{-8}$	$1,4 \cdot 10^{-8}$	$8 \cdot 10^{-9}$
Q $45°$, W:	$7,2 \cdot 10^{-8}$	$4,5 \cdot 10^{-8}$	$2,8 \cdot 10^{-8}$	$1,5 \cdot 10^{-8}$

*Commas in numbers indicate decimal points.

will be produced which is stronger by about a factor of 10^4 or 10^6. Also, the detector loads the thermal emission of the mirror optics by $1 \cdot 10^{-7}$ W at 230° K and ideal filtering. From Equation (18a), an additional noise power of about $3 \cdot 10^{-14}$ W/$\sqrt{Hz}$ follows from this. The problems of background suppression must be carefully solved and the first attempts are given in [8]. Using a time constant of the (alternating voltage) preamplifier, adapted to the modulation frequency of the optics, and a special measurement method in the signal processing, it seems possible to obtain a discrimination of the source signal from the "direct voltage" background.

For an optimum design of the bolometer itself, it is necessary to consider the relationship between the heat conduction value G and the time constant τ, the NEP and the permissible radiation load. Based on Equation (8), the total energy absorbed in the measurement element determines its temperature. However, Figure 5 shows that the temperature increased caused by Q_J has an optimum value as far as the detectibility sensitivity is concerned. One can immediately see that

$$G \approx 10 \cdot Q/T_B$$

(33)

should be the case. Q is, in practice, the sum of the electrical loss power Q_J and the background radiation Q_n. Because of the flat optimum, Q_J can increase up to this limit and still a Q_n, with the maximum of the same amount, is permissible without bringing about noticeable deterioration (effective bath temperature increased 10%) [12]. The background radiation which occurs for the required modulation frequency specifies the minimum value of G if the temperature of the cold bath is specified. Since noise is contained in Q_n according to Equation (18a), and on the other hand the NEP value of the detector is determined by G, we can establish the following relationship (ideal case) [8]:

/26

$$NEP = 6,4 \cdot (T_B/T_n)^{1/2} \cdot W_{Photon}$$

(34)

If the NEP value calculated in this way is smaller than the one from (1a), then the bolometer is not thermally overloaded. When filters are used, (34) no longer applies.

The previous relationships also show that an existing bolometer system is optimally designed by reducing the operational temperature alone. One does obtain an increase in the sensitivity but the detector becomes much faster because G now is over-dimensioned because of the rapidly decreasing heat capacity C, and the detectivity is worsened. In addition, the electrical resistance becomes too high. For optimal operational conditions, the heat conductivity value or the suspension of the crystal would have to be modified.

Conventional bolometer mountings include attaching the
crystal with two thin (typically 30 μm Au or Cu) wires, which
are used for heat conductors and electrical connections. With
a heat conductivity of $\lambda_{Au} \approx 1.5$ W cm^{-1} K^{-1} at 0.3° K (Handbook
of Physics and Chemistry E-10), the heat conductivity value is
calculated as follows for the one-dimensional case (length
$l \gg$ cross sectional area F)

$$G \approx \lambda \cdot F / l \qquad \text{WK}^{-1} \qquad (35)$$

l cannot be much over 1 cm for geometrical and mechanical
reasons. For thermal reasons, the mass of the wire should be
as small as possible (disturbing heat capacity). For G values
of 10^{-7} WK^{-1}, in this way one obtains very thin wires with a
diameter of only a few micrometers. Even if platinum is used
with an even poorer heat conductivity value, only a factor of
2 results. It would be thinkable to thermally couple the
element over its entire backside to the cold bath, using a
suitable substrate (thin adhesive layer?). This material would
have to have first class electrical insulation properties, as
well as a λ of typically 10^{-8} W cm^{-1} K^{-1}. Well-known epoxy
materials for cryogenic technology do not satisfy these
requirements, by far. In addition, in this case, because of
the (force) temperature gradient in the crystal, the current
densities are not equal — which complicates the relatively
simple relationships R(T), r(T), etc. For this reason, we will
not consider such an attachment technique.

The schematic structure of a complete conventional bolo-
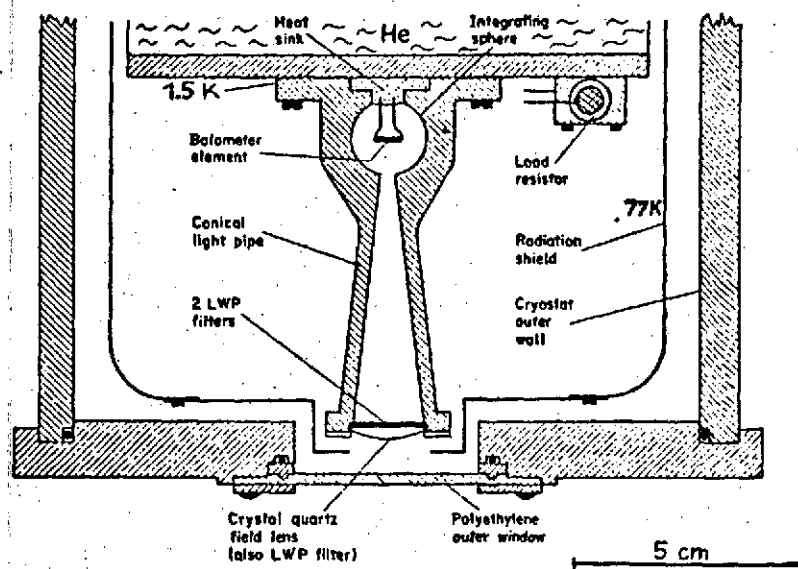meter system is shown in Figure 9.

Figure 9. Conventional bolometer system [14].

The planned application of the detector [8] (interferometry) does not allow the usual use of a conical light conductor piece, nor can the measurement element be suspended in a reflecting hollow sphere. The usual mounting of the crystal between two wires with a diameter of only 5 µm under tension would lead to technical difficulties.

In addition to undesirable piezo effects, unallowable oscillations can occur (optics). A relatively stable attachment method of the bolometer to a carrier which is simple to mount is planned, as shown in Figure 10. The internal part of the holder is electrically insulated from the external flange, but it is not thermally insulated because of its large surface area. The measurement element is subjected to no mechanical stress and is installed between two parallel stretched wires. The system can be directly screwed into the helium 3 vessel and a diaphragm system attached there is designed to hold away the undesirable background radiation from the detector, at a temperature of T ≈ 1° K.

/28

27

Pump line ———————

M = 1:1

Helium 3 vessel

Bolometer
holder

Bolometer

electrical
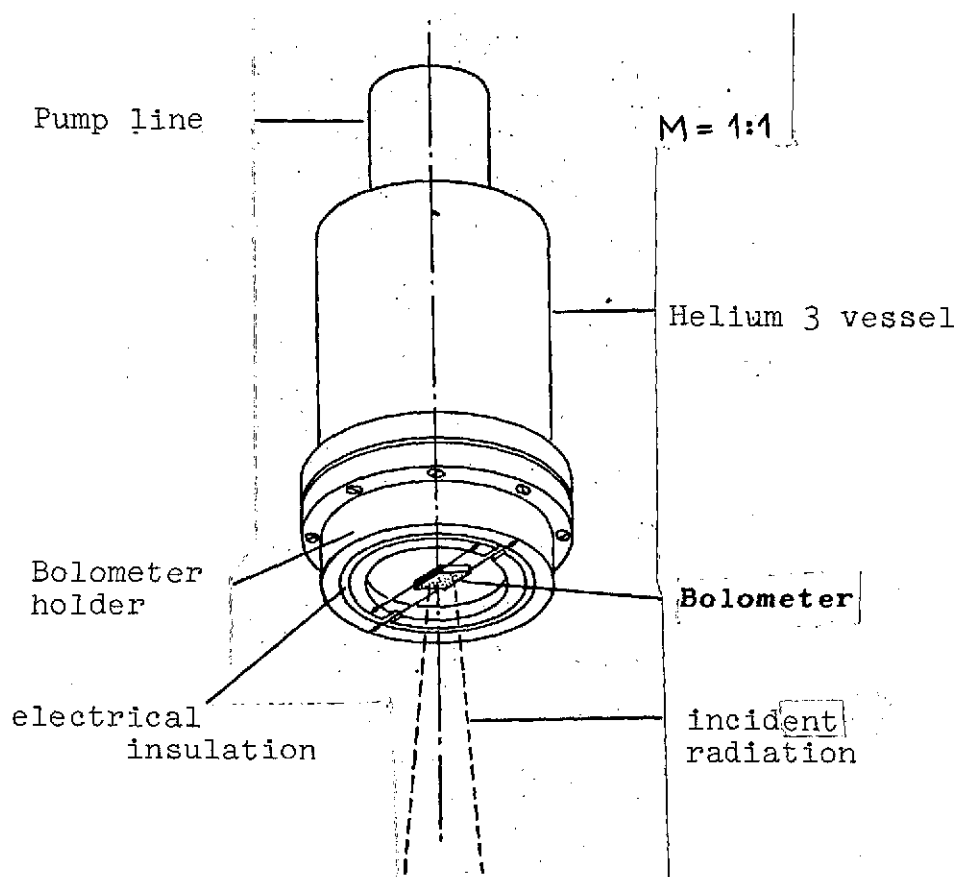insulation

incident
radiation

Figure 10. Planned bolometer support.

Table 3 shows the most important data on performance for
four different bolometers. The values of the best commercial
system (first column) are partially taken from [12] and
partially approximately calculated. The data for the other
detectors all are based on calculations.

6.   Helium-3 cryostat

It is relatively simple to provide a cold bath temperature
of about 1.5° K, as is required for previous bolometer systems.
This is done by reducing the vapor pressure in a vessel contain-
ing liquid He-4 to about 4.5 Torr (for example, atmospheric

TABLE 3

SPECIFIC DATA OF Ge BOLOMETERS SUITABLE FOR BALLOON EXPERIMENT

Detector	He-4 bolometer of Infrared Labs.	He-4 bolometer of IRL, cooled to the He-3 temperature	He-3 bolometer, adapted to telescope optics (own development)	He-3 bolometer, maximum possible values (own development)
Operational temperature, °K	1.5	0.3	0.3	0.3
Dimensions, mm	$\approx 0.7 \cdot 0.7 \cdot 0.4$	$\approx 0.7 \cdot 0.7 \cdot 0.4$	$3 \cdot 3 \cdot 0.5$	$1 \cdot 1 \cdot 0.5$
C, J/K	$\approx 6 \cdot 10^{-9}$	$\approx 5 \cdot 10^{-11}$	$1 \cdot 10^{-9}$	$1 \cdot 10^{-10}$
G, W/K	$1 \cdot 10^{-6}$	$\approx 2 \cdot 10^{-7}$	$9 \cdot 10^{-7}$	$1 \cdot 10^{-7}$
τ, s	$4 \cdot 10^{-3}$	$2 \cdot 10^{-4}$	$8 \cdot 10^{-4}$	$7 \cdot 10^{-4}$
$f_0 = \omega_k/2\pi$, Hz	40	1000	200	230
R, Ω	$\approx 5 \cdot 10^6$	$\approx 10^9$	$\approx 10^6$	$\approx 10^6$
Q atmosphere, W	35 km:$5 \cdot 10^{-8}$	40 km:$3 \cdot 10^{-8}$	40 km:$3 \cdot 10^{-8}$	45 km:$1.5 \cdot 10^{-8}$
NP atmosphere W/$\sqrt{Hz}$	$2 \cdot 10^{-14}$	$1.2 \cdot 10^{-14}$	$1.2 \cdot 10^{-14}$	$8 \cdot 10^{-15}$
Q optic, W	230 K: $1.5 \cdot 10^{-7}$	70K:$2.5 \cdot 10^{-9}$	70K:$2.5 \cdot 10^{-9}$	70K:$2.5 \cdot 10^{-9}$
NP optic, W/$\sqrt{Hz}$	$4 \cdot 10^{-14}$	$3 \cdot 10^{-15}$	$3 \cdot 10^{-15}$	$3 \cdot 10^{-15}$
NEP detector (1a),W/$\sqrt{Hz}$	$3 \cdot 10^{-14}$	$2 \cdot 10^{-15}$	$4 \cdot 10^{-15}$	$1.5 \cdot 10^{-15}$
NEP total W/$\sqrt{Hz}$	$5 \cdot 10^{-14}$	$1.3 \cdot 10^{-14}$	$1.3 \cdot 10^{-14}$	$9 \cdot 10^{-15}$

(Note in vertical text spanning Q atmosphere through NEP total rows: at filter with 20 μm cut-on)

pressure at a flight altitude of 35 km), which results in the desired temperature reduction. Because of the fact that the vapor pressure of He-4 is too small, and because of losses through the superfluid He II film, under practical conditions, it is not possible to operate at a temperature below about 1.1° K. In order to reach the required range of 0.3° K, it is necessary to use helium-3 [16].

In addition to the considerably higher vapor pressure of He-3 compared with He-4 (see Figure 11), there is an additional advantage in that He-3 has a considerably greater specific heat below 1° K than the metals used in the cryostat, so that the cooling of the corresponding materials is not made so difficult. When constructing such cryostats, it is necessary to make sure that the total amount of gas required does not become too large, because one normal liter of He-3 costs DM 500. If the filling amounts are about 6 Nl, one can have an operational period between 10 and 20 hours, depending on the incident heat to the He-3 vessel, typically 10 µW. In the present application for bolometer cooling, the operation of a pure He-3 vaporizer is sufficient. The adiabatic mixing and separation process of liquid He-3 and superfluid He-4 (He-3/He-4 mixing cryostat) only brings about significant advantages above 0.3° K (see Figure 12). The increased molar specific heat of He-3/He-4 compared with pure He-3 brings about a negative mixing enthalpy.

Within the operating range of a He-3 cryostat, the cooling performances are essentially determined by the suction power of the pumps used. The vapor pressure corresponding to 0.3° K is $2 \cdot 10^{-3}$ Torr, and for a heat load of 50 µW, a suction power of 20 liters per second results, which can be achieved with a Hg diffusion pump nominally rated at 80 liters per second. The use of such a pump for bolometer cooling is described in [2].
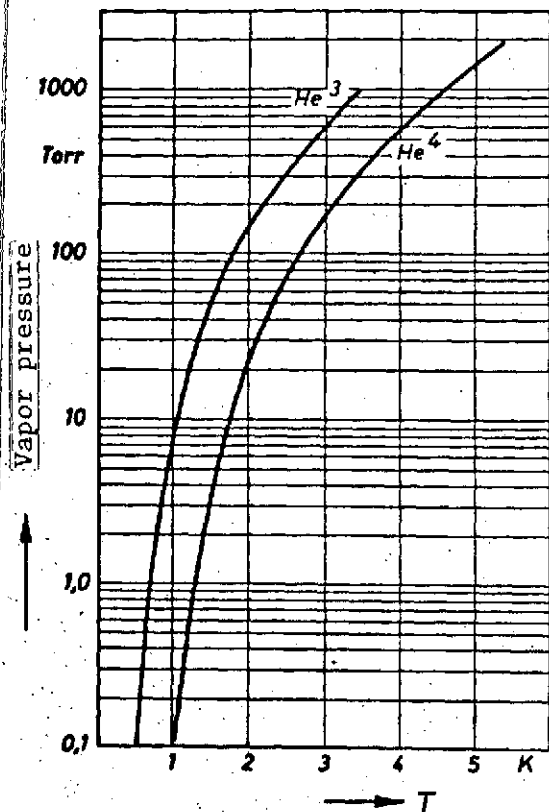
Figure 11.   Vapor pressures
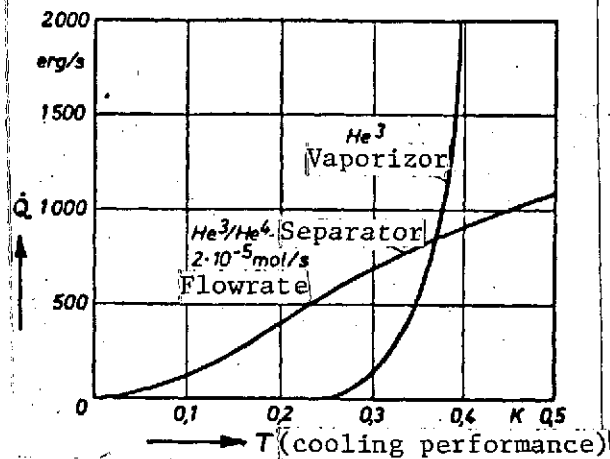of He 3 and He 4 [16].

Figure 12.   Cooling performances
which can be achieved with the
same pump sizes [16].

Except for the high electrical
energy consumption, we also had
disturbing acoustic feedbacks
to the bolometer, which were
expressed by an increase in the
noise level.   Accordingly, such
a pumping system cannot be used
for the planned balloon experiment.   For the first time, we will /33
attempt to use a He-3 cryostat with an adsorption pump for
cooling an IR bolometer.

The particular advantages associated with the adsorption
of He-3 in activated charcoal or zeolith within a He-3 cryostat
are the following:

— no diffusion pump is required,

— pressure decreases in the pumping lines are absent;

— the cooling power which can be achieved is higher than with external pumps and there is no shaking,

— there is no electrical power requirement.

Compared with zeolith, activated charcoal has a reduced water adsorption capacity. Per gram, a surface area of about 1200 m^2 are available, and the concave surfaces of the storage pores $(\phi \approx 10 \text{ Å})$ bring about the desired vapor pressure reduction, i.e., adsorption [17]. Since the adsorption capacity depends on temperature, by varying the charcoal temperature, it is possible to control the resulting suction power or to bring about the desorption of the adsorbed gas by a correspondingly high temperature. Figure 13 shows the adsorption amounts of He-3 for various charcoal temperatures.

Experience on the construction and operation of a He-3 cryostat with adsorption pump are available [18]. Such a system is shown in Figure 14. Various test devices and auxiliary units (pumps, etc.) are attached to the cryostat itself (see Figure 15), for the planned laboratory investigations using various bolometers and filters. A working cycle occurs as follows: after precooling the two radiation protective coverings to the temperature of liquid N_2 or liquid He-4, the inner He-4 container is pumped down to about 1.2° K (about /34 0.6 Torr). The heat conduction of the He-4 gas surrounding it (exchange gas, a few Torr) cools all parts of the He-3 system. Now the helium 3 gas introduced from the external He-3 handling system can condense at pressures of > 20 Torr at the 1.2° K walls, and collects in the lowest He-3 vessel (approximately 15 cm^3). The charcoal pump is located at the upper end of the cryostat and has approximately the N_2 temperature. According to Figure 13, all of the He-3 is desorbed. After ending the
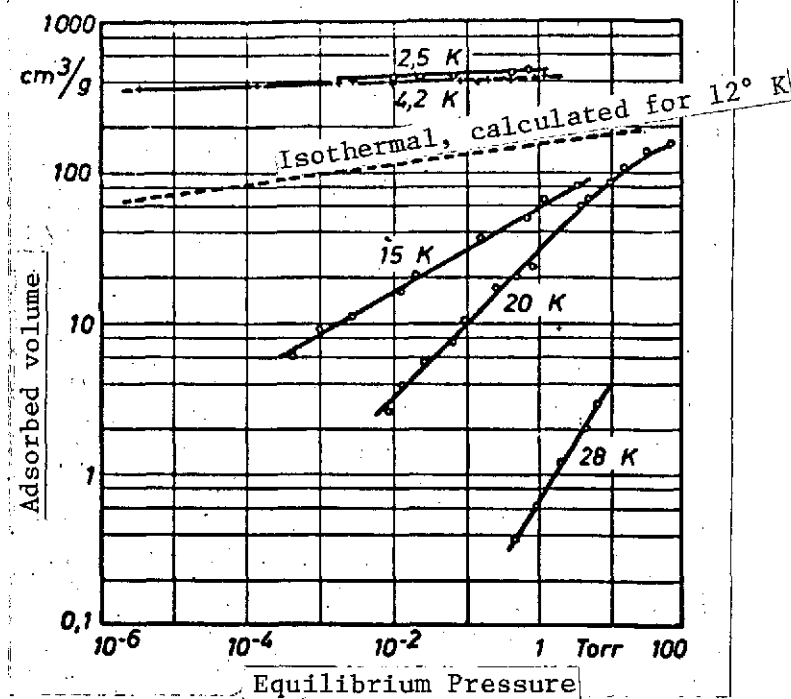
Figure 13. Adsorption of He 3 in Supersorbon B 16 activated charcoal [16].

condensation process (< 1 h), first of all the temperature is reduced to about 0.5° K (0.2 Torr), by externally pumping down the He-3. Then, the charcoal pump is brought into contact with the 1.2° K bath, which then introduces the action of the pump. Until there is a reduction to 0.3° K, about 35% of the liquid He-3 vaporizes and the remainder is now available for the "measurement interval," a time of about 15 hours. In /35 the meantime, the activated charcoal attached to the He-3 vessel has automatically produced the required insulation vacuum of < 10^{-6} Torr. The temperature of the charcoal pump does not have to be maintained at 1.2° K; according to Figure 13, the suction power does not vary too much for T < 4° K. The only important thing is a guarantee for a good removal of the condensation heat which occurs (typically one Joule per cycle)

Manometer

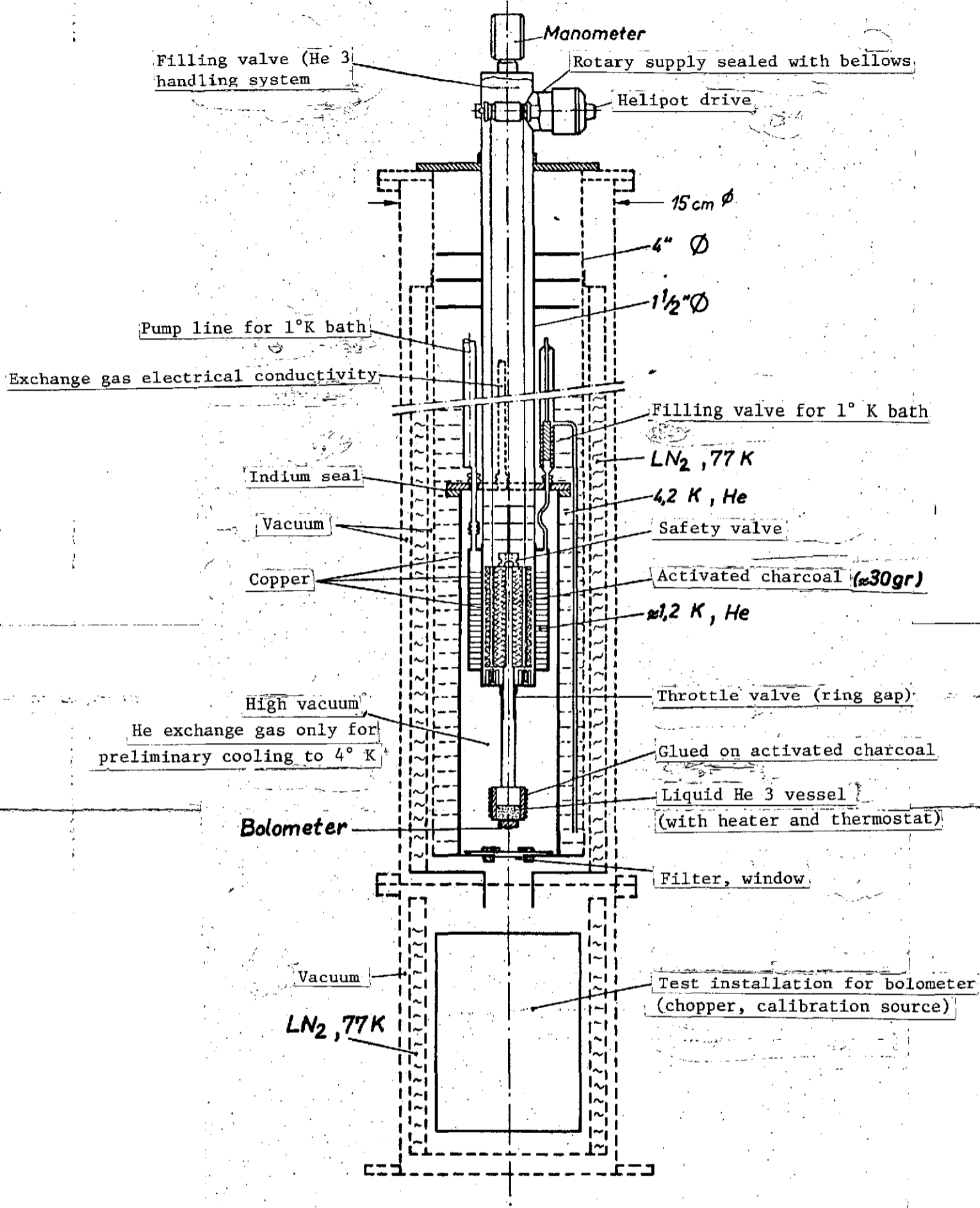Filling valve (He 3 handling system

Rotary supply sealed with bellows

Helipot drive

15 cm ∅

4" ∅

1½" ∅

Pump line for 1°K bath

Exchange gas electrical conductivity

Filling valve for 1° K bath

LN_2, 77 K

4,2 K, He

Indium seal

Safety valve

Vacuum

Activated charcoal (≈30gr)

Copper

≈1,2 K, He

High vacuum

He exchange gas only for preliminary cooling to 4° K

Throttle valve (ring gap)

Glued on activated charcoal

Liquid He 3 vessel (with heater and thermostat)

Bolometer

Filter, window

Vacuum

Test installation for bolometer (chopper, calibration source)

LN_2, 77 K

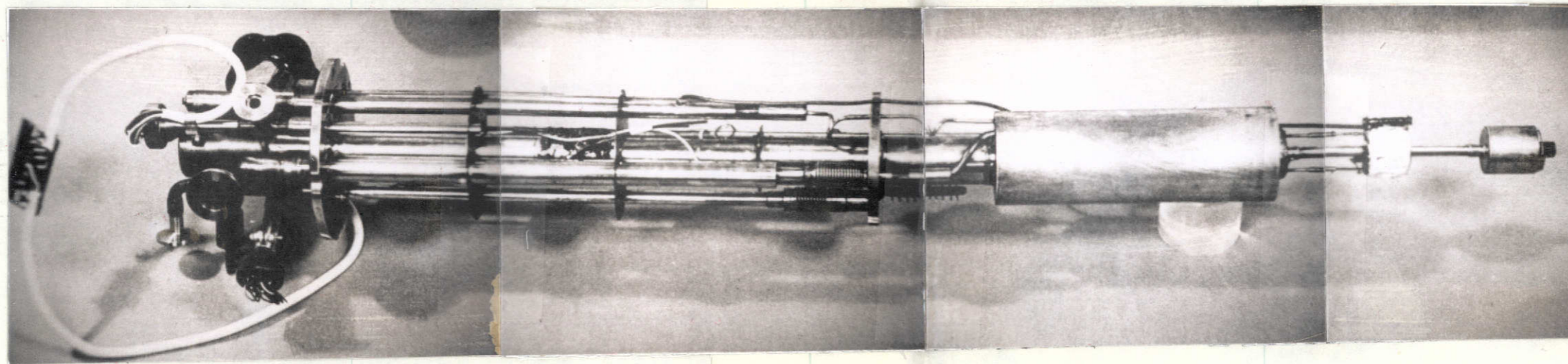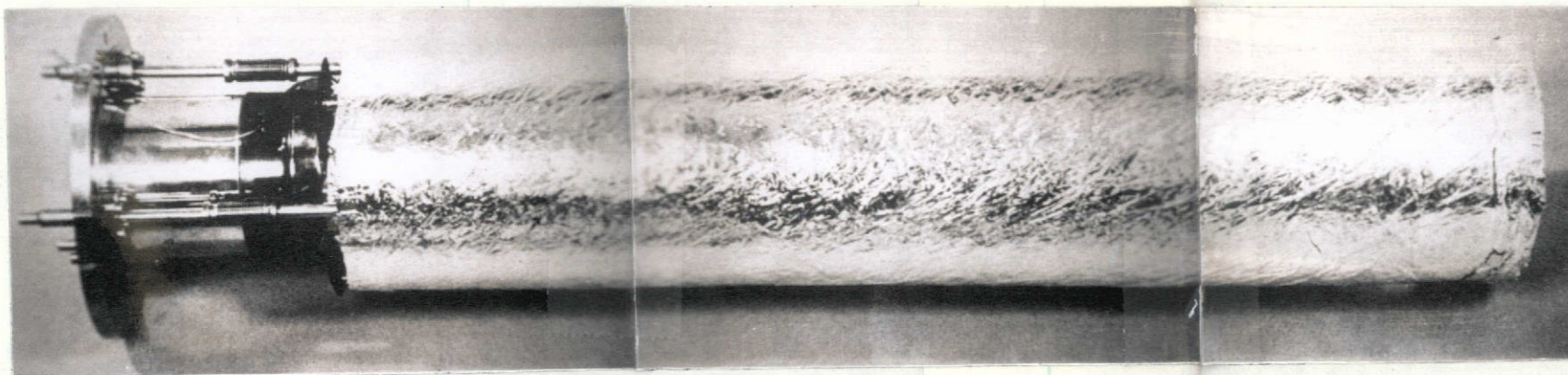Figure 14.   Principle diagram of a He 3 cryostat with adsorption pump.

Figure 15. He 3 cryostat

35

to the He-4 bath. The bath temperature of 0.3° K can probably
be maintained using an electrical heater and the corresponding
measurement and control loop to an accuracy of 10^{-3}° K.
Therefore, one becomes free of fluctuations in the suction
power or influences by tipping the measurement unit. The
remaining "signal voltages" at the bolometer exceed the
measurement signal proper by about 10^3, but from a measurement
point of view, they only have to belong to the category
"direct voltage." When the cooling period is over, then the
He 3 adsorbed by the charcoal pump can again be desorbed by
"heating" to T > 40° K. If there is no equalization vessel
connected to the He-3 system, then there will be a pressure
increase to several atmospheres.

A special version of the He-3 cryostat will be used for
the balloon experiment. The minimum dimensions of 60 cm length
and 12 cm diameter cannot be violated because of the thermo-
dynamics and because of technical factors. Also, the minimum
weight is 10 kg.

7. References

1.   Naumann, F., and K. W. Michel. High Resolution IR
      Spectral Photometry with a Balloon Telescope. MPI-
      PAE/TB Extraterr., Vol. 9, October, 1973.

2.   Drew, H. D., and A. J. Sievers. A He-3 Cooled Bolometer
      for the Far Infrared. Applied Optics, Vol. 8, No. 10,
      October, 1969.

3.   Chanin, G. Liquid Helium Cooled Bolometers. In:
      Infrared Detection Techniques for Space Research.
      D. Reidel Publishing Company, 1972.

4.   Coron, N., et al. A New Type of Helium Cooled Bolometer.
      In: Infrared Detection Techniques for Space Research.
      D. Reidel Publishing Company, 1972.

5.⁴. Nayar, P. S. A New Far Infrared Detector. Infrared
      Physics, Vol. 14, 1974, p. 31.

6.   Jantsch, O., and I. Feigt. The Noise in Semiconductors.
      Physik in unserer zeit, Vol. 2, 1972.

7.   Boyle, W. S., and K. F. Rogers. Performance Characteris-
      tics of a New Low-Temperature Bolometer. J. of the
      Optical Society of America, Vol. 49, No. 1, January,
      1959.

8.   Hofmann, R. The Optical System of a Balloon Telescope
      for High Resolution IR Spectroscopy. MPI-PAE Diploma
      Thesis, August, 1974.

9.   Armstrong, K. R., and F. J. Low. New Techniques for
      Far Infrared Filters. Applied Optics, Vol. 12, No.
      9, September, 1973.

10.   Low, F. J. Low Temperature Germanium Bolometer. J. of
      the Optical Society of America, Vol. 51, No. 11,
      November, 1961.

11.   Hawks, K. H. A Radiometric Investigation of Emissivities   /39
      and Emittances of Selected Materials at Cryogenic
      Temperatures. Ph.D. Tesis, Purdue University, 1969.

12.   Low Temperature Germanium Bolometer. Data sheet of
      Infrared Laboratories, Inc., Tucson, Arizona, 1974.

13.   Zwerdling, S., and J. P. Theriault. Far Infrared
      Spectral Properties of Compensated Ge and Si. Infrared
      Physics, Vol. 12, 1972, p. 165.

14.   Zwerdling, S., R. A. Smith, and J. P. Theriault. A Fast
      High Responsivity Bolometer Detector for the Very Far
      Infrared. Infrared Physics, Vol. 8, 1968, p. 271.

15.   Drapatz, S. Infrared Atmospheric Transmission and Emission
      at Balloon Altitudes. MPI-PAE/TB Extraterr., No. 13,
      August, 1974.

16.   Wiedemann, W. Extrem tiefe temperaturen-grundlagen,
      messtechnik und anwendungen, lehrgangshandbuch
      kryotechnik (Extreme Low Temperatures — Fundamentals,
      Measurement Technology, and Applications, Cryogenic
      Handbook). Duesseldorf, VDI-Verlag, April, 1973.

17. Schuetz, H. Activated Charcoal. Klima-Kaelte-Technik, April, 1974.

18. Wiedemann, W., and E. Smolic. A Hermetically Sealed He-3 Cryostat with a Charcoal Adsorption Pump. Proc. IInd. Int. Cryogenic Engineering Conference, Brighton, 1968.